

2020-09-11

Diffusion rather than intraflagellar transport likely provides most of the tubulin required for axonemal assembly in *Chlamydomonas*

Julie Craft Van De Weghe
University of Georgia

Et al.

Let us know how access to this document benefits you.

Follow this and additional works at: https://escholarship.umassmed.edu/radiology_pubs



Part of the Algae Commons, Amino Acids, Peptides, and Proteins Commons, Cell Biology Commons, Cellular and Molecular Physiology Commons, and the Developmental Biology Commons

Repository Citation

Craft Van De Weghe J, Harris JA, Kubo T, Witman GB, Lechtreck KF. (2020). Diffusion rather than intraflagellar transport likely provides most of the tubulin required for axonemal assembly in *Chlamydomonas*. Radiology Publications. <https://doi.org/10.1242/jcs.249805>. Retrieved from https://escholarship.umassmed.edu/radiology_pubs/563

This material is brought to you by eScholarship@UMassChan. It has been accepted for inclusion in Radiology Publications by an authorized administrator of eScholarship@UMassChan. For more information, please contact Lisa.Palmer@umassmed.edu.

RESEARCH ARTICLE

Diffusion rather than intraflagellar transport likely provides most of the tubulin required for axonemal assembly in *Chlamydomonas*

Julie Craft Van De Weghe^{1,¶,*}, J. Aaron Harris^{1,¶,‡}, Tomohiro Kubo^{2,§}, George B. Witman² and Karl F. Lechtreck¹

ABSTRACT

Tubulin enters the cilium by diffusion and motor-based intraflagellar transport (IFT). However, the respective contribution of each route in providing tubulin for axonemal assembly remains unknown. Using *Chlamydomonas*, we attenuated IFT-based tubulin transport of GFP- β -tubulin by altering the IFT74N-IFT81N tubulin-binding module and the C-terminal E-hook of tubulin. E-hook-deficient GFP- β -tubulin was incorporated into the axonemal microtubules, but its transport frequency by IFT was reduced by ~90% in control cells and essentially abolished when the tubulin-binding site of IFT81 was incapacitated. Despite the strong reduction in IFT, the proportion of E-hook-deficient GFP- β -tubulin in the axoneme was only moderately reduced. *In vivo* imaging showed more GFP- β -tubulin particles entering cilia by diffusion than by IFT. Extrapolated to endogenous tubulin, the data indicate that diffusion provides most of the tubulin required for axonemal assembly. We propose that IFT of tubulin is nevertheless needed for ciliogenesis, because it augments the tubulin pool supplied to the ciliary tip by diffusion, thus ensuring that free tubulin there is maintained at the critical concentration for plus-end microtubule assembly during rapid ciliary growth.

KEY WORDS: Flagella, Cilia, Microtubule, Axoneme, Calponin homology domain, IFT81, IFT74, Diffusion

INTRODUCTION

Tubulin is the main protein of the axoneme, the structural core of cilia and flagella (Borisy and Taylor, 1967). The microtubules of the axoneme provide the scaffold to anchor dynein arms and other protein complexes and serve as tracks for intraflagellar transport (IFT). During ciliary assembly, vast amounts of tubulin move from the cell body, the place of tubulin synthesis, into the organelle. For example, a 12- μ m long axoneme, as it is typical for *Chlamydomonas*, which we used in this study, contains ~350,000 tubulin dimers (Bhogaraju et al., 2014). Studies in several species have revealed that tubulin enters cilia by both IFT and diffusion (Craft et al., 2015; Hao et al., 2011; Luo et al., 2017).

During IFT, arrays of IFT particles (IFT trains) are moved distally and proximally along the axonemal microtubules by means of the motor proteins kinesin and IFT dynein, respectively. These IFT trains carry ciliary building blocks, such as tubulin and axonemal dyneins, into the growing organelle (Cole et al., 1998; Kozminski et al., 1993). IFT speed and frequency are similar in growing and non-growing cilia, but the frequency of tubulin transport is upregulated while cilia elongate and attenuated in non-growing cilia, indicating tight control of delivery of tubulin to the cilium by IFT (Craft et al., 2015).

Much less is known about diffusion of tubulin into the cilium. Diffusion into the cilium of proteins and complexes larger than ~50 kDa is severely restricted by the ciliary gate formed by the transition zone, and it is thought that association with IFT enables such proteins and complexes to pass through the ciliary gate (Awata et al., 2014; Breslow et al., 2013; Kee et al., 2012; Lin et al., 2013). Indeed, the absence of IFT cargo adapters and mutation of the cargo binding sites on IFT particles largely diminishes the presence of the respective cargoes from cilia, indicating that they critically depend on IFT for ciliary entry and accumulation (Ahmed et al., 2008; Badgandi et al., 2017; Berbari et al., 2008; Dai et al., 2018; Hou and Witman, 2017; Hunter et al., 2018). However, tubulin, presumably in a form no smaller than the 110-kDa α -tubulin- β -tubulin dimer, diffuses into cilia, and this diffusion occurs in both growing and fully formed cilia (Craft et al., 2015; Harris et al., 2016; Kee and Verhey, 2013). Tubulin entry into cilia by diffusion continues when IFT is switched off using the temperature-sensitive kinesin-2 mutant *fla10-1* (Craft et al., 2015). Spatial mapping showed that ~30% of all GFP-tubulin enters full-length primary cilia by diffusion through the lumen of the axonemal cylinder (Luo et al., 2017). To determine the respective contributions of IFT and diffusion in supplying tubulin for axonemal assembly, we manipulated IFT-tubulin interactions to attenuate tubulin supplied by the IFT route.

In vitro interaction studies revealed that the N-terminal domains of the IFT particle proteins IFT74 and IFT81 form a bipartite tubulin-binding module (Bhogaraju et al., 2013). In detail, the calponin homology (CH) domain of IFT81 binds to the globular cores of the α -tubulin- β -tubulin dimer, providing specificity. The basic N terminus of IFT74 likely binds the acidic C-terminal E-hook of β -tubulin, stabilizing the IFT-tubulin interaction. To test the role of the IFT74N-IFT81N tubulin-binding module *in vivo*, Kubo et al. (2016) expressed IFT74 Δ 130, which lacks the tubulin-interacting N-terminal 130 residues of IFT74, and IFT81-CH5E, in which five basic residues in the IFT81 CH domain were replaced with glutamate to abolish tubulin-IFT interaction, in corresponding *ift74-2* and *ift81-1* null mutants (Bhogaraju et al., 2013; Brown et al., 2015). However, *Chlamydomonas* expressing IFT81-CH5E or IFT74 Δ 130 still assemble near full-length cilia, albeit at reduced rates (Kubo et al., 2016). In both mutants, transport of GFP- α -tubulin by IFT is reduced, potentially explaining the delay in ciliary

¹Department of Cellular Biology, University of Georgia, Athens, GA 30602, USA.

²Department of Cell and Developmental Biology, University of Massachusetts Medical School, Worcester, MA 01655, USA.

*Present address: Department of Pediatrics, University of Washington, Seattle, WA 98195, USA. †Present address: Bowdoin Group, Waltham, MA 02451, USA.

[‡]Present address: Department of Anatomy and Structural Biology, University of Yamanashi, Kofu, Japan.

[¶]These authors contributed equally to this work

**Author for correspondence (lechtrek@uga.edu)

 J.C., 0000-0002-4492-6089

Handling Editor: David Stephens

Received 4 June 2020; Accepted 31 July 2020

growth. A double mutant (*ift74-2 IFT74Δ130 ift81-1 IFT81-CH5E*) assembles severely truncated cilia with an otherwise normal ultrastructure, supporting the notion that the IFT74N-IFT81N module promotes ciliogenesis by facilitating IFT transport of tubulin (Kubo et al., 2016). Although great care was taken to ensure that the above-described manipulations of IFT81 and IFT74 were specifically affecting tubulin transport, defects in IFT itself cannot be excluded. The strain expressing the N-terminally truncated IFT74, for example, displays anomalies in IFT speed and frequency, and the abundance of various IFT proteins in the cell body is altered (Brown et al., 2015). Further, phospholipase D is enriched in the cilia, indicative of defects in retrograde IFT (Brown et al., 2015; Lehtreck et al., 2013). Due to the short length of the cilia, IFT could not be assessed directly in the double mutant. It is therefore of interest to analyze how changes in tubulin itself affect its transport by IFT. Here, we focused on the E-hook of β -tubulin, which, as noted above, has been predicted to interact with the N-terminal domain of IFT74.

In the ciliate *Tetrahymena thermophila*, genomic replacement of wild-type β -tubulin with versions lacking a functional E-hook severely impairs cell viability and ciliary assembly (Duan and Gorovsky, 2002; Xia et al., 2000). Thus, approaches altering the entire tubulin pool of a cell are unsuited to determine the specific effect of such manipulations on tubulin transport by IFT. Here, we expressed GFP-tagged α - and β -tubulins in *Chlamydomonas* to levels of $\sim 10\%$ of the total tubulin and analyzed how the altered E-hooks affect IFT transport without perturbing either IFT itself, IFT of the endogenous tubulin, or ciliary assembly. This approach has the potential to shed light on the relative contributions of IFT

and diffusion in ciliary tubulin supply by revealing how a reduction in IFT of a specific assembly-competent GFP-tagged tubulin derivative affects its share in the axoneme.

We show that deletion of the E-hook of β -tubulin severely reduces its ability to bind to IFT trains. Nevertheless, E-hook-deficient β -tubulin remained abundant in the axoneme, suggesting a smaller than anticipated role of IFT in providing tubulin for axonemal assembly. Although our results reveal that most of the tubulin for axonemal assembly is supplied by diffusion, we postulate that tubulin transport by IFT ensures that enough soluble tubulin is available near the ciliary tip to promote axonemal elongation and ciliary growth.

RESULTS

The E-hook of β -tubulin promotes tubulin-IFT interaction *in vivo*

Superfolder GFP (GFP) was fused to the N terminus of β -tubulin and expressed in wild-type *Chlamydomonas* (Fig. 1). Western blotting using anti-GFP and anti- β -tubulin confirmed expression and the presence of GFP- β -tubulin in cilia, and we observed a similar ratio between tagged and untagged tubulin in the whole-cell and cilia samples (Fig. 1A). Live-cell imaging showed that GFP- β -tubulin is incorporated into both cytoplasmic and axonemal microtubules (Fig. 1B). As previously reported for GFP- α -tubulin, IFT of GFP- β -tubulin was rarely observed in full-length cilia but occurred with high frequency in growing cilia obtained by first deciliating the cells using a pH shock (Fig. 1C) (Craft et al., 2015). Therefore, the transport frequencies for all tubulin constructs used in this study were obtained using regenerating cilia with a length of $\sim 4\text{--}9\ \mu\text{m}$. A comparison of strains expressing different

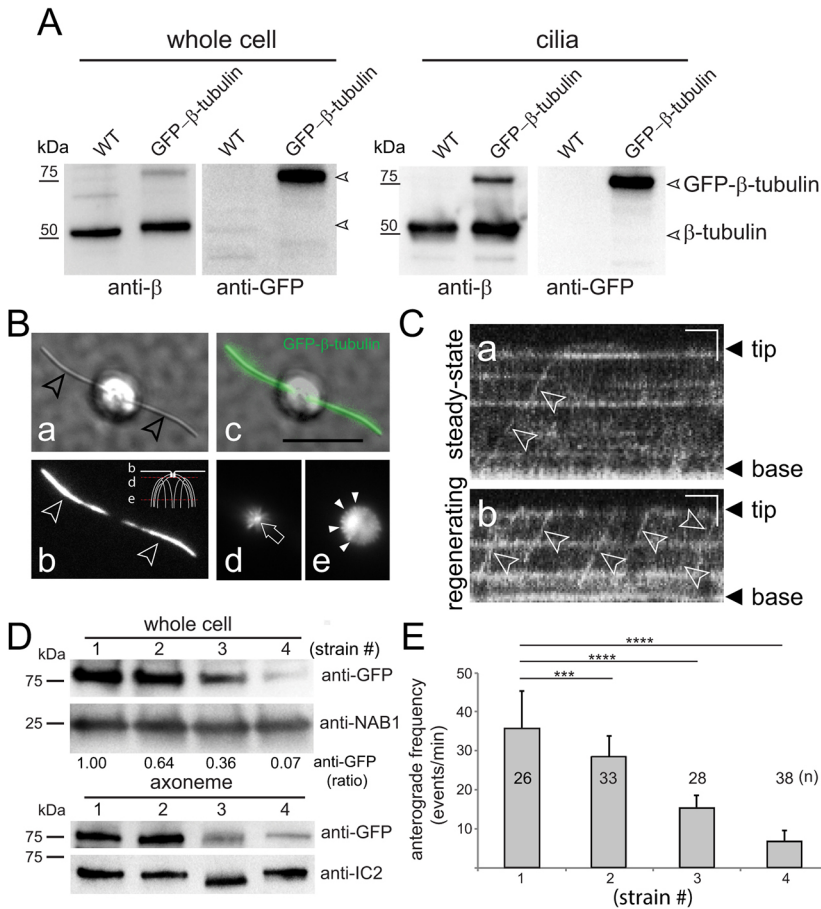


Fig. 1. GFP- β -tubulin is transported by IFT and incorporated into microtubules. (A) Western blot analysis of whole cells and isolated cilia from a wild-type strain expressing GFP- β -tubulin and an untransformed control strain (WT). Western blots were probed with a polyclonal antibody to β -tubulin and with anti-GFP; the position of endogenous β -tubulin, the GFP-tagged version, and marker proteins are indicated. (B) Live-cell imaging of a cell expressing GFP- β -tubulin in DIC (a) and low-angle illumination (b, d, e); an overlay image of a and b is shown in c. The still images present a focal series showing the level of the cilia (marked by arrowheads in a and b), the basal bodies (arrow in d) surrounded by the root microtubules, and the cortical microtubules of the cell body (arrowheads in e). The diagram in b indicates the different focal planes. Scale bar: 10 μm . (C) Kymograms showing IFT transport (arrowheads) of GFP- β -tubulin in full-length (a) and regenerating (b) cilia. The tip and the base of the cilia are indicated. Scale bars: 2 s (horizontal) and 2 μm (vertical). (D) Western blots of whole-cell and axoneme samples obtained from four wild-type strains (numbers 1–4) expressing different levels of GFP- β -tubulin. Blots were stained with anti-GFP; antibodies to the cell body protein nucleic acid binding protein 1 (NAB1) and the axonemal dynein intermediate chain 2 (IC2) were used as loading controls for the cell body and axonemes, respectively. For quantitation of the whole cell:axoneme anti-GFP ratio, the intensity of the GFP-tubulin band in the highest expressing strain was set to 1.00; all values were corrected for the anti-NAB1 and anti-IC2 signals. (E) Frequency of GFP- β -tubulin anterograde transport during ciliary regeneration in the strains shown in Fig. 1D. Data are mean \pm s.d. The significance based on a two-tailed *t*-test is indicated (****P* < 0.001; *****P* < 0.0001).

amounts of tagged β -tubulin revealed an approximately linear correlation between the total amount of GFP- β -tubulin expressed, the frequency of its IFT transport in regenerating cilia, and its share in the axoneme (Fig. 1D,E).

To investigate the role of the E-hook of β -tubulin (β E-hook) in IFT of tubulin, GFP-tagged β -tubulin was modified by replacing the β E-hook with the E-hook of α -tubulin (α E-hook), by replacing five glutamic acid residues in the E-hook with alanine to undermine charged-based interactions (-5 E-hook), and by deleting of the C-terminal 13 residues (Δ E-hook; Fig. 2, Table S1). Cells expressing the transgenic GFP-tubulins grew normally, showed wild-type motility, assembled full-length cilia at normal rates, and IFT of tubulin progressed at standard velocities (Table S1, data not shown). To determine whether the E-hook modifications affected the frequency of GFP- β -tubulin transport, we selected strains expressing similar amounts of the transgenes, as determined by western blotting of whole-cell samples (Fig. 2A). For all four constructs, $\sim 8\%$ of the total GFP-tagged protein was in the cilia and $\sim 90\%$ of the ciliary GFP-tubulin was in the axonemal fraction, indicating that the fusion proteins entered cilia and were assembly competent (Fig. 2B). All three mutations in the β E-hook resulted in significant reductions in the frequency of anterograde tubulin IFT, with the Δ E-hook construct being the most affected with a $\sim 90\%$ reduction in anterograde IFT (2.4 events/min, s.d. 2.9 events/min, $n=98$ cilia analysed compared to 21 events/min, s.d. 14.3 events/min, $n=85$ for wild-type β -tubulin; Fig. 2C).

Loss of the β E-hook weakens the interaction of tubulin with IFT *in vitro* (Bhogaraju et al., 2013), so we investigated how loss of the β E-hook affects the processivity of tubulin transport in cilia. IFT transport of GFP- α -tubulin mostly ($\sim 98\%$) proceeds in one run to the tip, indicative of a stable interaction with IFT trains (Craft et al.,

2015). Similarly, 97% ($n=559$ IFT events) of transport events involving wild-type GFP- β -tubulin proceeded nonstop to the tip of the elongating cilia. In contrast, such processive IFT events were reduced by 25–45% for the constructs with modified E-hooks (Fig. 2D,E). In those strains, GFP- β -tubulin was observed converting from IFT transport to diffusion, indicative of a dissociation from IFT (Fig. 2D).

Considering the apparent importance of the β E-hook for tubulin binding to IFT, we transplanted the E-hook and neighboring regions of β -tubulin onto GFP or mNeonGreen (mNG; Fig. S1A). Similar to GFP alone, the GFP- and mNG- β E-hook fusion proteins readily entered cilia by diffusion. Whereas IFT transport of GFP alone was not observed, GFP- and mNG- β E-hook fusions underwent anterograde IFT, albeit at extremely low frequencies (<0.05 events/min) indicating a rather weak binding to IFT trains (Fig. S1B). In summary, the β E-hook is neither sufficient nor necessary for IFT transport; its loss, however, reduces the frequency and processivity of tubulin transport, supporting the view that the β E-hook stabilizes IFT-tubulin interactions.

High frequency transport of tubulin by IFT requires the E-hook of β -tubulin

Bhogaraju et al. (2013) proposed that tubulin binding by IFT trains involves the CH domain of IFT81 and an interaction between the E-hook of β -tubulin and the N-terminal domain of IFT74 (Fig. 3A). To further investigate the validity of this model, we analyzed tubulin transport in *ift81-1 IFT81-CH5E*, an *ift81* null mutant expressing a variant IFT81 in which five basic residues (K73, R75, R85, K112 and R113) in the CH domain critical for tubulin binding were replaced with glutamates, and in *ift74-2 IFT74 Δ 130*, an *ift74* null mutant rescued with a version of IFT74 lacking the proposed

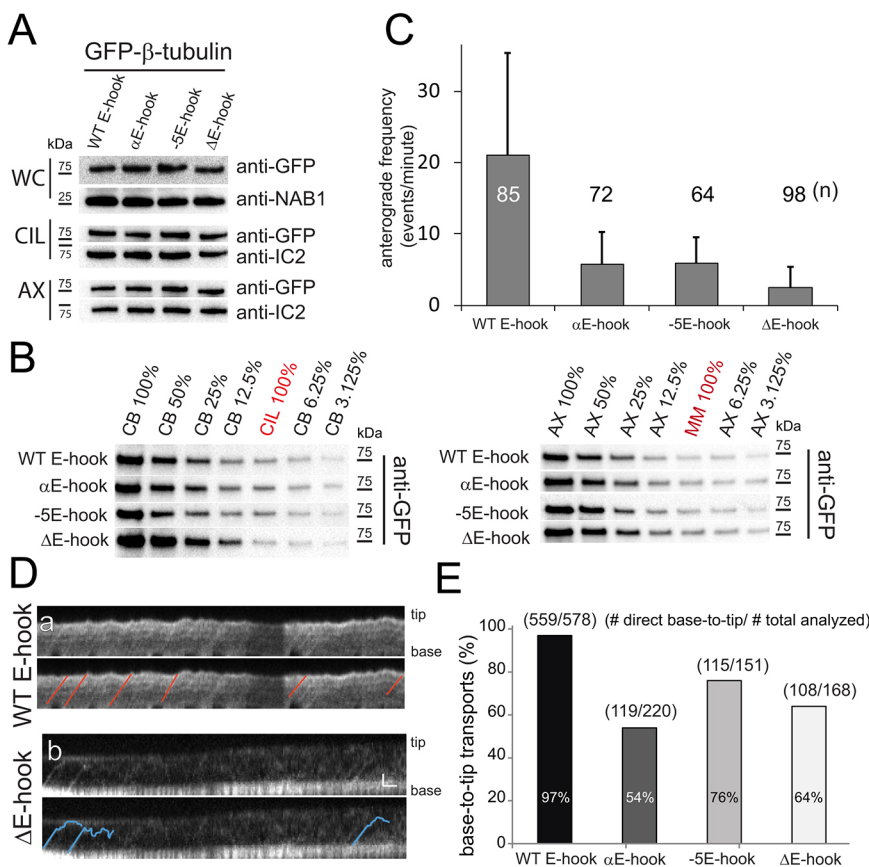


Fig. 2. The E-hook of β -tubulin promotes transport by IFT. (A) Western blot analyses of whole cells (WC), isolated cilia (CIL), and axonemes (AX) from strains expressing GFP- β -tubulin with wild-type and modified E-hooks. Anti-GFP was used to visualize the tagged β -tubulins; antibodies to NAB1 and IC2 were used to visualize loading controls for WC and CIL/AX, respectively. (B) Left and right panels show western blots of dilution series comparing the amount of GFP- β -tubulin in the deciliated cell bodies (CB) to that in cilia (CIL), and the amount of GFP- β -tubulin in the axonemes (AX) to that in the detergent-soluble membrane and matrix fraction (MM), respectively. A value of 100% indicates that equivalents of the two fractions were loaded (i.e. one cell body per two cilia). (C) The average frequency of anterograde IFT events observed for the GFP-tagged β -tubulins. The number of regenerating cilia analyzed for each strain (n) and the s.d. are indicated. (D) Kymograms showing transport of full-length (WT E-hook) and E-hook-deficient (Δ E-hook) β -tubulin in regenerating cilia. Selected tracks are marked on the lower duplicate panel for each strain. Note the reduced frequency and reduced run length of transport events involving the truncated GFP- β -tubulin (blue lines). Scale bars: 1 s (horizontal) 1 μ m (vertical). (E) The percentage of IFT events that proceeded nonstop from ciliary base to tip for wild-type (WT E-hook) and modified GFP- β -tubulins. The number of processive base-to-tip events and the total number of events analyzed are indicated.

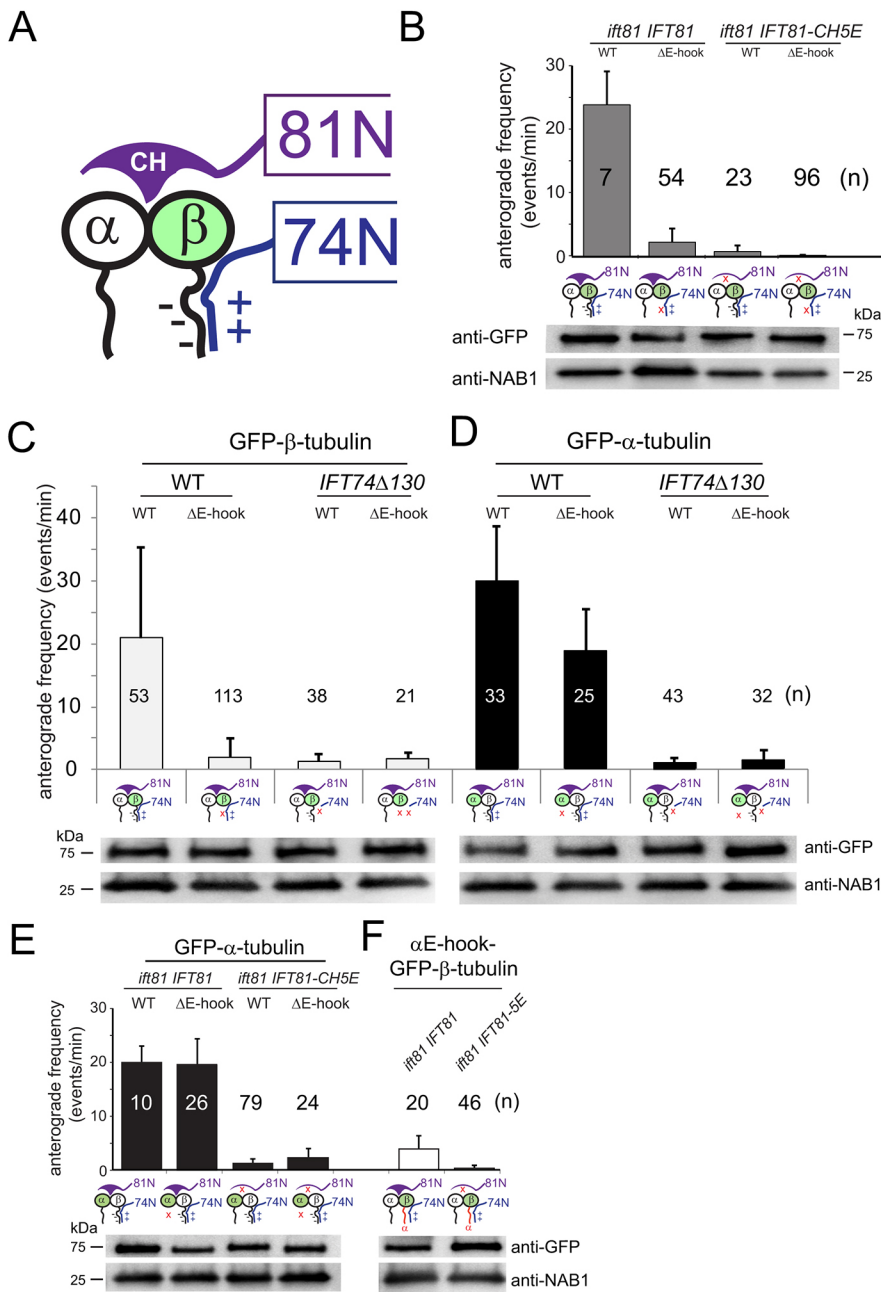


Fig. 3. Loss of the E-hook attenuated IFT of GFP- β -tubulin. (A) Schematic presentation of tubulin binding by the IFT74N-IFT81N module (as proposed by Bhogaraju et al., 2013). (B) The frequency of anterograde IFT events observed for full-length (WT) and truncated (Δ E-hook) GFP-tagged β -tubulins in cilia of the *ift81-1 IFT81* and the *ift81-1 IFT81-CH5E* strains. The number of regenerating cilia analyzed for each strain (*n*) is indicated. Data are mean+s.d. The corresponding western blot comparing the amounts of wild-type and Δ E-hook GFP- β -tubulin in whole-cell samples of the strains is shown below the graph. Tagged tubulin was detected with anti-GFP, anti-NAB1 staining was used to verify equal loading. (C,D) Anterograde transport of full-length and E-hook-deficient GFP- β -tubulin (C) and GFP- α -tubulin (D) in the *ift74-2 IFT74 Δ 130* strain and wild-type (WT) controls. Data are mean+s.d., and *n* for each strain is indicated. Western blots of whole-cell samples documenting similar expression of the transgenes are below. (E) Frequency of anterograde IFT for full-length and E-hook-deficient GFP- α -tubulin in the *ift81-1 IFT81* and the *ift81-1 IFT81-CH5E* strains. Data are mean+s.d., and *n* for each strain is indicated. The corresponding western blots of the whole-cell samples of these strains are shown below the graph. (F) Anterograde transport of α E-hook-GFP- β -tubulin in the *ift81-1 IFT81* and the *ift81-1 IFT81-CH5E* strains. Data are mean+s.d., and *n* for each strain is indicated. The corresponding western blots of the whole cell samples are shown. Diagrams in B–F depict the mutations in tubulin, IFT74 and IFT81 in each strain.

N-terminal tubulin-binding domain (Fig. 3B–F) (Bhogaraju et al., 2013; Brown et al., 2015; Kubo et al., 2016).

The E-hook-deficient β -tubulin is predicted to be unable to interact with the N-terminal domain of IFT74 and, thus, its binding to IFT trains should depend on the CH domain of IFT81. In the *ift81-1 IFT81-CH5E* background, strongly reduced transport frequencies were observed for full-length β -tubulin, whereas anterograde IFT of Δ E-hook β -tubulin was essentially abolished (\sim 1% compared to full-length β -tubulin in strains with wild-type IFT81; Fig. 3B). Sporadic transport of E-hook-deficient β -tubulin in *ift81-1 IFT81-CH5E* could be due to residual binding by IFT81-CH5E or low capacity binding elsewhere on the IFT train. The *ift74-2 IFT74 Δ 130* strain lacks the proposed β E-hook-binding site of IFT74. The anterograde IFT frequencies of full-length and E-hook-deficient β -tubulin were similarly low in this strain, suggesting that both bind with similar strength to IFT trains presumably via the

remaining IFT81-CH site (Fig. 3C). Thus, the lack of the N-terminal region of IFT74 renders IFT unable to discriminate between full-length and E-hook-deficient β -tubulin.

We wondered whether IFT transport specifically requires the E-hook of β -tubulin or whether the E-hook of α -tubulin also contributes to IFT. In wild-type IFT cells, transport of E-hook-deficient α -tubulin was somewhat reduced but still occurred at a high frequency when compared to the transport of E-hook-deficient β -tubulin (Fig. 3D,E). Also, strains expressing *ift74-2 IFT74 Δ 130* or *ift81-1 IFT81-CH5E* transported full-length and E-hook-deficient α -tubulin with similar, albeit low frequencies (Fig. 3D, E). Thus, the IFT system is largely insensitive to the loss of the α E-hook. Furthermore, substitution of the E-hook of GFP- β -tubulin with that of α -tubulin did not support normal transport frequencies in wild type or the *ift81-1 IFT81-CH5E* background (Figs 2C and 3F). The data support the model proposed by Bhogaraju et al.

(2013) in which the E-hook of β -tubulin interacts with the N-terminal domain of IFT74.

Near abrogation of IFT of GFP- β -tubulin only moderately reduces its axonemal presence

Tubulin enters cilia by diffusion as well as IFT (Craft et al., 2015; Luo et al., 2017). The expression of a tagged assembly-competent tubulin with strongly decreased binding to IFT allowed us to assess the respective contributions of IFT and diffusion in supplying tubulin for axonemal assembly. If, for example, $\sim 90\%$ of the ciliary tubulin were delivered by IFT, one would expect that a strong reduction in IFT of a specific tubulin species would be reflected by a similarly strong reduction of its share in the axoneme. Towards this end, we analyzed the correlation between the frequency of IFT and the axonemal share for full-length and E-hook-deficient GFP- β -tubulin (Fig. 4). Loss of the β E-hook reduced the frequency of IFT by $\sim 90\%$ in wild type (Figs 3C and 4A), the *ift81-1 IFT81* strain (expressing a wild-type IFT81 transgene; Fig. 3B), and the *ift81-1 IFT81-CH5E* strain (Fig. 3B), each in comparison to full-length GFP- β -tubulin in the same background. Western blot analyses of axonemes, however, documented only a moderate reduction of E-hook-deficient GFP- β -tubulin compared to the full-length version (Figs 2A and 4B; Fig. S2A,B). Quantitative analysis of western blots from nine independent cilia isolates (four, three and two in the wild-type (Fig. 4C), *ift81 IFT81* (Fig. S2C), and *ift81-1 IFT81-CH5E* (Fig. S2C) backgrounds, respectively) showed an average reduction of $\sim 17\%$ (s.d. 35%) for truncated versus full-length GFP- β -tubulin. Western blotting of isolated axonemes using anti- β -tubulin confirmed that full-length and truncated GFP- β -tubulin were present in similar ratios to the endogenous β -tubulin (Fig. 4D); for this experiment we used a polyclonal anti-*Chlamydomonas*- β -tubulin because most commercial antibodies to β -tubulin react with the E-hook (Silflow and Rosenbaum, 1981). Even in the near absence of transport by IFT, as observed for E-hook-deficient GFP- β -tubulin in the *ift81-1 IFT81-CH5E* strain ($\sim 99\%$ reduction in frequency in comparison to GFP- β -tubulin in wild type; Fig. 3B), the truncated GFP-tagged tubulin was still well represented in the cilia (Fig. S2D; $n=2$ independent isolates). In live-cell imaging, the cilia of cells expressing full-length GFP- β -tubulin (in the *ift20 IFT20-mCherry* background to facilitate identification) and of cells expressing E-hook-deficient GFP- β -tubulin were of similar brightness (Fig. 4E). In summary, the strong reduction in the frequency of IFT of E-hook-deficient β -tubulin is not matched by a proportional reduction of its presence in the axoneme.

Our data suggest a limited quantitative contribution of IFT in providing tubulin for axonemal assembly. However, cells with defects in the IFT74N–IFT81N tubulin-binding module largely fail to assemble cilia. We therefore considered possible alternative mechanisms that could potentially explain the surprisingly limited effect that the reduction in IFT frequency of the truncated β -tubulin had on its presence in the axoneme.

First, if retrograde IFT had a higher affinity for endogenous full-length β -tubulin than for truncated GFP- β -tubulin, the latter could become enriched in the cilium. The frequencies of retrograde tubulin traffic, however, were negligibly low compared to anterograde traffic and were similar in range for full-length GFP- β -tubulin and its derivatives (Fig. S2E,F).

Second, the total amount of GFP- β -tubulin tolerated in axonemal microtubules could be limited, and even low IFT frequencies as observed for truncated GFP- β -tubulin could still be sufficient to saturate GFP- β -tubulin incorporation. In this case, there might not be a difference in the amount of full-length GFP- β -tubulin versus

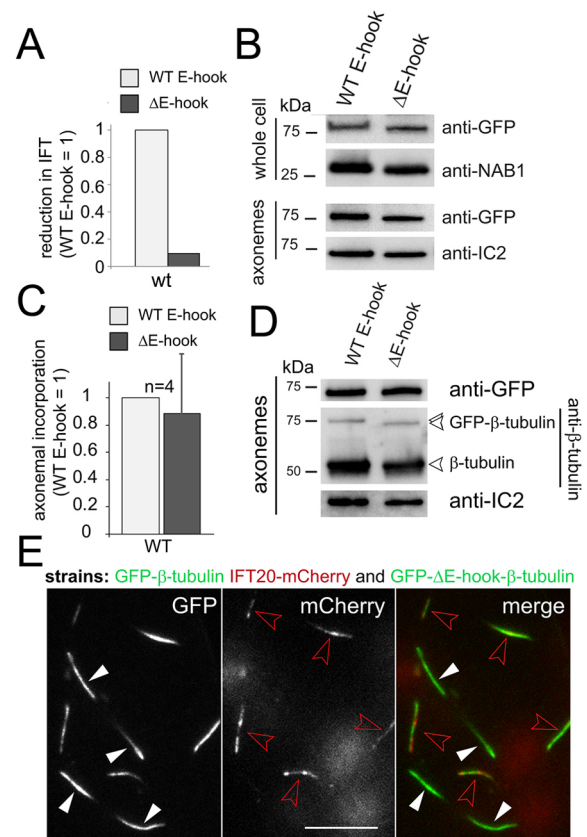


Fig. 4. Abated IFT of E-hook-deficient tubulin does not cause a proportional reduction of its presence in the axoneme. (A) The reduction in IFT transport of truncated (Δ E-hook) versus full-length (WT E-hook) β -tubulin in control cells. The frequency observed for the full-length GFP- β -tubulin was set to 1. See Fig. 3C for the original data, s.d. and n values. (B) Western blot of control cells, comparing whole-cell and axoneme samples of the indicated strains using anti-GFP and antibodies to NAB1 and IC2, as loading controls. (C) Bar chart showing the change in the axonemal amounts of E-hook-deficient (Δ E-hook) versus full-length β -tubulin in control cells, as deduced from western blots probed with anti-GFP. The band intensity of the full-length GFP- β -tubulin was set to 1. n , number of independent cilia isolates. Data are mean \pm s.d. (D) Western blot comparing isolated axonemes from a wild-type strain expressing full-length or truncated β -tubulin stained with anti-GFP, anti- β -tubulin, and anti-IC2. (E) TIRF images showing the GFP and mCherry signals in cilia of live cells. Cells expressing E-hook-deficient GFP- β -tubulin (white arrowheads) and cells expressing full-length GFP- β -tubulin in the *ift20-1 IFT20-mCherry* background (red arrowheads) were mixed to allow for a comparison of the GFP-signal strength with the same microscope settings. Scale bar: 10 μ m.

E-hook-deficient GFP- β -tubulin incorporated into the axoneme. We consider this situation unlikely, because the IFT frequency and axonemal quantity of full-length GFP- β -tubulin correlated well over a wide range of expression levels (Fig. 1D,E).

Third, different ciliary growth rates could be accompanied by distinct contributions of IFT and diffusion to axonemal assembly. Indeed, reduced transport of GFP- β -tubulin correlates with slow ciliary elongation (Kubo et al., 2016). In our experiments, we used regenerating cilia to determine IFT frequency of GFP- β -tubulin, whereas cilia assembled postmitotically in the course of the normal cell cycle were used for our biochemical analyses. Regenerating cilia require ~ 90 min to grow 12 μ m, whereas postmitotic assembly is considerably slower, taking ~ 4 h to build an ~ 8 - μ m long cilium (Madey and Melkonian, 1990; Rosenbaum et al., 1969). Therefore, postmitotic ciliary assembly could involve less IFT and more diffusion of precursors, potentially explaining the high share

of Δ E-hook GFP- β -tubulin in cilia despite its low frequency of IFT. Western blot analysis, however, did not reveal a significant difference in the share of full-length and E-hook-deficient β -tubulin in postmitotic versus regenerated axonemes (Fig. S2G).

Fourth, E-hook-deficient β -tubulin could incorporate into the axoneme at a significantly higher rate than the full-length protein. In this case, one would expect the E-hook deficient version to be more abundant in the axoneme than full-length GFP- β -tubulin under conditions when both proteins show the same frequency of IFT, as is the case in the *ift74-2 IFT74 Δ 130* background, when tubulin transport relies solely on the CH domain of IFT81. However, analysis of *ift74-2 IFT74 Δ 130* axonemes revealed similar amounts of full-length and truncated GFP- β -tubulin (Fig. S2H). In conclusion, our observations are explained best by assuming that IFT transports only a fraction of the tubulin present in the axoneme and that most tubulin enters cilia by diffusion.

Diffusional entry of GFP- β -tubulin particles into cilia outnumbers entry via IFT

If entry by diffusion provides more tubulin for axonemal assembly than IFT, the number of GFP- β -tubulin particles entering cilia by diffusion should exceed those entering via IFT. To estimate tubulin influx, we bleached and imaged full-length and growing cilia of a wild-type strain expressing GFP- β -tubulin at high laser intensities until individual GFP- β -tubulin particles became visible (Fig. 5A). Because diffusing GFP- β -tubulin moves swiftly, identifying single

particles required movies to be recorded at 20–40 frames per second (f.p.s.; compared to 10 f.p.s. for standard recordings); high laser intensities prevented unbleached soluble GFP- β -tubulin from re-accumulating in the ciliary matrix, which would obscure individual particles (Fig. 5B). In addition to the random back-and-forth motion typical of free diffusion, some GFP- β -tubulin particles moved unidirectionally for extended distances toward the tip or base of the cilia with velocities exceeding those of IFT ($\geq 10 \mu\text{m/s}$; Fig. 5B, red arrows). A similar behavior was previously described for EB1-mNG movements in cilia and could represent non-random diffusion (Harris et al., 2016). In the most proximal region of the cilium, high-frequency entry of GFP- β -tubulin mostly by diffusion generated a dense signal, often preventing a reliable particle count; for scoring, we used a more distal region, in which individual tracks were typically resolved (Fig. 5C; Fig. S3A, Movie 1).

GFP- β -tubulin entry by IFT occurred at frequencies of 1.7 particles/min and 24.2 particles/min into full-length and regenerating cilia, respectively, whereas entry by diffusion into full-length and regenerating cilia was observed at an average of 108 particles/min and 101 particles/min, respectively (Fig. 5D; Fig. S3A). In addition to the frequency of IFT, determining the number of GFP- β -tubulin cargoes per train is critical for assessing GFP- β -tubulin influx via IFT. IFT trains encompass on average ~ 50 IFT-B complexes and each IFT train provides multiple binding sites for tubulin (Jordan et al., 2018). However, most GFP- β -tubulin particles moving by IFT bleached in one or two steps, indicating the

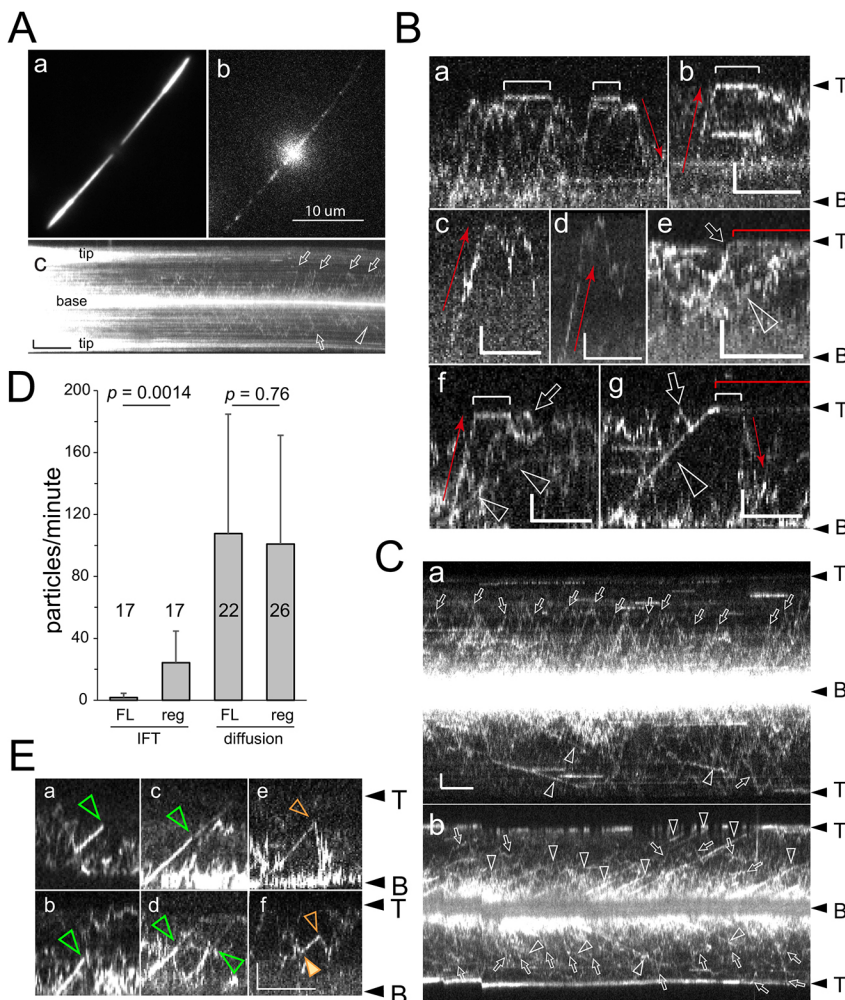


Fig. 5. GFP- β -tubulin rapidly enters cilia by diffusion. (A) Still images (a, b) of a wild-type cell expressing GFP- β -tubulin with full-length cilia prior (a) and during bleaching (b). The corresponding kymogram (c) shows how diffusion (arrows) and IFT (arrowhead) of GFP- β -tubulin become apparent as axonemal GFP- β -tubulin is bleached. Scale bars: 2 s (horizontal) and 2 μm (vertical). The movies were recorded at 40 f.p.s. (B) Gallery of kymograms showing diffusion (white arrows) and IFT (arrowheads) of GFP- β -tubulin in bleached full-length (a–d) and regenerating (e–g) cilia. A subset of GFP- β -tubulin diffusion occurs rapidly and almost unidirectional along the cilia (red arrows). At the ciliary tip, diffusing GFP- β -tubulin becomes transiently immobilized (indicated by white brackets); more stable association is visible in panels e and g (indicated by red brackets). Scale bars: 2 s (horizontal) 2 μm (vertical). (C) Kymograms of bleached full-length (a) and regenerating (b) cilia showing the entry of GFP- β -tubulin into cilia by diffusion (arrows) and IFT (arrowheads). Note accumulation of GFP- β -tubulin at the tip of growing cilia. Scale bars: 2 s (horizontal) 2 μm (vertical). (D) Frequency of GFP- β -tubulin entry by IFT and diffusion in regenerating (reg) and full-length (FL) cilia. The standard deviation, number of cilia analyzed and probability value (P) based on a two-tailed t -test are indicated. (E) Kymograms of GFP- β -tubulin moving by IFT in a growing cilium. GFP photobleaching events are marked by green arrowheads; bleaching appears to occur in one (a,b) or two steps (c,d). Loading (filled arrowhead in f) and unloading (open arrowheads in e and f) of GFP- β -tubulin from IFT is indicated. Based on movies recorded at 20 f.p.s. Scale bars: 2 s (horizontal) 2 μm (vertical). In B,C,E: T, position of cilia tip; B, position of cilia base.

presence of just one or two GFPs per train (Fig. 5E panels a–d). Furthermore, the brightness of GFP–tubulin moving by IFT was typically in a range similar to that of the faster-moving diffusing particles, which is particularly apparent when GFP– β -tubulin particles switch from IFT to diffusion and vice versa (Fig. 5E panels e and f). We conclude that each IFT train carries only one or a few GFP– β -tubulin particles. GFP– β -tubulin is expressed to \sim 10% of the total β -tubulin level (Figs 1A and 4D). Therefore, based on the above observations, we estimate that \sim 17 tubulin dimers/s enter cilia by diffusion compared to \sim 4–8 dimers/s by IFT at peak entry rates. Of note, the IFT frequency of GFP–tubulin declines progressively as cilia get longer, whereas its entry by diffusion continues at high frequency in full-length cilia (Fig. 5C,D; Craft et al., 2015). Although the dense traffic of GFP–tubulin in cilia allowed only an approximation of tubulin influx, the imaging data strongly support the hypothesis that more tubulin enters cilia by diffusion than by IFT.

Tubulin entering the cilium by diffusion rapidly reaches the tip and is incorporated into the axoneme

IFT moves tubulin processively to the ciliary tip and releases it near the growing end of the axoneme, which could increase the chance of incorporation into the axoneme when compared to tubulin entering cilia by diffusion, which likely moves freely through the transition zone and therefore is expected to exit the cilium at a similar rate as it enters if it is not captured by a microtubule end. To analyze the behavior of tubulin near the ciliary tip, we bleached only the tip region using a focused laser beam and imaged GFP– β -tubulin re-entering the bleached region (Fig. S3B–D; Movie 2).

In full-length cilia, diffusing GFP– β -tubulin particles often became stationary at the ciliary tip for \sim 0.3–3.3 s (average 0.77 s, s.d. 0.8 s, $n=16$) likely indicating transient assembly into the axoneme (Fig. 5B). Interestingly, in a subset of cilia, two GFP–tubulin dots spaced \sim 600 nm apart recovered near the ciliary tip, likely indicating limited turnover at the ends of both the A-tubule and the slightly shorter B-tubule (Fig. S3B) (Ringo, 1967). Overall, the incorporation of GFP– β -tubulin into the tip of full-length cilia was limited, as previously reported for mCherry– α -tubulin (Fig. 5C panel a; Fig. S3C panels a and b) (Harris et al., 2016).

A more pronounced recovery of the tip signal was observed in growing cilia reflecting axonemal growth (Fig. 5C panel b; Fig. S3C panels c and d). Recovery of the signal at the tip of growing cilia was also observed in cells expressing E-hook-deficient β -tubulin (Fig. S3B panel d). In growing cilia, one or more diffusing GFP– β -tubulin particles typically entered the bleached tip region prior to the arrival the first GFP–tubulin particle via IFT (Fig. 5B panels e–g; Fig. S3D). GFP– β -tubulin particles approaching the tip of growing cilia by IFT or diffusion remained mobile, dwelled transiently or remained stationary until the signal was bleached (Fig. 5B); the latter putatively indicates incorporation into the axoneme (Fig. 5B panels e and g; Fig. S3C,D). Thus, GFP– β -tubulin moving by both IFT and diffusion appeared to be added to the ciliary tip, indicating that both routes contribute to axonemal assembly.

DISCUSSION

Tubulin enters cilia by diffusion and as a cargo of IFT. The latter is regulated in a ciliary-length-dependent manner and it is likely that this regulation of tubulin influx contributes to ciliary length control (Craft et al., 2015; Hao et al., 2011; Kubo et al., 2016). To explore the respective contributions of each route in providing tubulin for axonemal assembly, we manipulated tubulin IFT by taking

advantage of the detailed knowledge of IFT–tubulin interactions. Previously, *in vitro* studies showed that the E-hook of β -tubulin confers stable binding of tubulin dimers to the IFT81N–IFT74N module by interacting with IFT74 (Bhogaraju et al., 2013). In agreement with this model, removal of the E-hook of GFP-tagged β -tubulin reduced the frequency of its transport by IFT by \sim 90%. However, the strong reduction in IFT was not mirrored by a comparative reduction of the share of the tagged E-hook-deficient β -tubulin present in cilia. We propose that the predominant role of IFT with regard to tubulin is to elevate intraciliary tubulin concentration, especially near the tip of the growing cilium, rather than to provide the bulk of tubulin needed for ciliary assembly.

IFT74 specifically interacts with the β -tubulin E-hook to promote tubulin IFT

Bhogaraju and colleagues (2013) showed that tubulin-binding by the IFT74N–IFT81N module was significantly reduced when the E-hook of β -tubulin was removed by a brief subtilisin treatment. Subtilisin treatment only mildly affected tubulin binding by IFT81N alone, suggesting that the positively charged IFT74N interacts with the negatively charged E-hook of β -tubulin. Our *in vivo* observations support this model and provide the following additional insights: (1) The E-hook of β -tubulin is not essential for binding to IFT trains or incorporation into the axonemal microtubules; it is also not sufficient to support IFT of fusion cargoes. (2) IFT74N's interaction with tubulin is specific for the β -tubulin tail, whereas the negatively charged E-hook of α -tubulin is expendable. (3) GFP–tubulin transport was essentially abolished when the deletion of the β E-hook was combined with mutations in IFT81N, an arrangement thought to disrupt both interactions of the IFT74N–IFT81N module with tubulin. This suggests that the IFT74N–IFT81N module is the major tubulin-binding site on anterograde IFT trains and argues against the presence of additional tubulin-binding sites independent of the IFT74N–IFT81N module (Bhogaraju et al., 2014). This statement is supported by the recent finding from Kubo et al. (2016) that double mutants in IFT74N and IFT81N are essentially unable to assemble cilia.

The bulk of axonemal tubulin is supplied by diffusion

Complete replacement of endogenous β -tubulin with versions lacking the E-hook or possessing mutated E-hooks has been shown to interfere with cell division and axonemal assembly (Nielsen et al., 2001; Thazhath et al., 2002). Here, we circumvented problems resulting from the loss of endogenous β -tubulin by expressing small amounts of GFP-tagged tubulin derivatives in cells possessing endogenous wild-type tubulin. This approach allowed us to analyze IFT transport of tagged modified tubulins independently of ciliary assembly. Surprisingly, a strong reduction in IFT of E-hook-deficient GFP– β -tubulin was not matched by a proportional reduction of its share in the axoneme, suggesting that a large portion of GFP– β -tubulin enters the cilium by diffusion. However, because the axonemes of our transgenic strains are composed mostly of endogenous tubulin, it raises the question of whether results for the tagged tubulins are representative of tubulin in general. Direct editing of the endogenous tubulin genes has not yet been achieved in *Chlamydomonas*, preventing us from testing whether the tagged tubulins are fully functional, i.e. would support cell viability and axonemal assembly in the absence of wild-type tubulin. In budding yeast, α -tubulin with a C-terminal GFP tag is not able to replace endogenous tubulin, although co-expression is tolerated (Carminati and Stearns, 1997; Huh et al., 2003). Because of such issues, complementation assays for tagged tubulins are

rarely executed. Although we cannot exclude a functional restriction, we note that N-terminally GFP-tagged α - and β -tubulin are incorporated into multiple types of microtubules in *Chlamydomonas*, that their expression apparently does not affect microtubule-based processes or cell viability, and that GFP- α -tubulin undergoes acetylation and polyglutamylation in cilia (Craft et al., 2015). Given that GFP- β -tubulin appears to function like endogenous β -tubulin in these ways, it is reasonable to assume that it serves as a good proxy for the endogenous tubulin in axonemal assembly. We conclude that, in *Chlamydomonas*, most of the tubulin used for axonemal assembly enters the cilium by diffusion. Similarly, Luo and colleagues (2017) reported that ~30% of EGFP- α -tubulin enters full-length primary cilia through the center of the axoneme by diffusion, with additional diffusion events probably occurring outside of the axonemal cylinder, where IFT trains move (Luo et al., 2017).

Estimates of the tubulin transport capacity of IFT support this notion. Although several other IFT proteins possess CH domains, only those of IFT81 and IFT54 bind tubulin, and the CH-domain of IFT54 is expendable for ciliary assembly (Bhogaraju et al., 2014; Taschner et al., 2016; Zhu et al., 2017). Thus, it is likely that the IFT74N-IFT81N module forms, or is part of, the only high-capacity tubulin-binding site of IFT. An average-length anterograde IFT train (~300 nm) contains ~50 IFT-B complexes, and ~60 IFT trains enter a regenerating cilium each minute (Dentler, 2005; Jordan et al., 2018). Although not shown experimentally, the low stability of small tubulin oligomers suggests that the transported form of tubulin is an α - β dimer. Under these assumptions, and assuming that every train is completely loaded, IFT could transport ~60% of the tubulin required to assemble a 10- μ m long axoneme in 60 min and about a third of the ~9000 tubulin dimers required each minute during rapid ciliary growth (~350 nm/min; Bhogaraju et al., 2014). Apparently, the IFT pathway simply lacks the capacity to be the major provider of axonemal tubulin during rapid ciliary assembly. Also, the photobleaching kinetics and brightness of GFP- β -tubulin while moving by IFT indicate that the trains are only partially loaded with tubulin. Our fluorescence recovery after photobleaching (FRAP) analysis revealed that this shortfall is made up for by a continuous high-frequency influx of GFP-tubulin by diffusion, which occurs in both growing and full-length cilia [this study and Craft et al. (2015)].

In full-length cilia, IFT transport of GFP-tubulin was rarely observed, and tubulin particles appear to associate only transiently to the axonemal plus end (Harris et al., 2016). Thus, IFT appears to have a limited role as a tubulin carrier during the maintenance of full-length *Chlamydomonas* cilia. However, significant tubulin exchange at the tip has been observed in zygotic cilia of *Chlamydomonas*, indicating that these are more dynamic than those of vegetative cells (Marshall and Rosenbaum, 2001), and in primary cilia of *Caenorhabditis elegans* (Hao et al., 2011). In the latter, FRAP analysis revealed fast incorporation of YFP-tagged tubulin β -4 at the ends of the middle and distal segments, suggesting that both the A- and the B-tubules undergo dynamic length changes largely driven by IFT-based tubulin transport (Hao et al., 2011).

A capture-and-carry model for tubulin transport by IFT

IFT is known to be essential for cilia assembly. It transports tubulin into cilia, and defects in the IFT74N-IFT81N tubulin-binding module reduce the ciliary growth rate or impair ciliogenesis, indicating that tubulin transport by IFT is critical for the assembly of *Chlamydomonas* cilia (Bhogaraju et al., 2013; Kubo et al., 2016). How can these observations be reconciled with the data presented here suggesting that most tubulin enters cilia by diffusion? Similar to the assembly of sperm flagella in *Drosophila*, apicomplexan

parasites such as *Plasmodium* rapidly assemble numerous axonemes within the cell body cytoplasm of the mother cell without IFT, because IFT genes are absent in *Plasmodium* (Billker et al., 2002; Briggs et al., 2004; van Dam et al., 2013). Apparently, diffusion is sufficient to provide the tubulin necessary for axonemal assembly in these situations, as is generally assumed to be the case for other large-scale microtubule-based structures such as the mitotic spindle. Thus, axonemal assembly per se does not require IFT of tubulin. It seems likely that the geometry of projecting cilia, especially the narrowness of their connection to the cell body cytoplasm and their small volume, could explain IFT's importance in ciliogenesis. In *Chlamydomonas*, the opening into the cilium corresponds to just ~0.01% of the surface of the plasma membrane and the cross-sectional area available for diffusion through the transition zone is likely to be substantially less due to the doublet microtubules and numerous other structures present in the transition zone (Ringo, 1967). As a result, the transition zone will function as a passive physical barrier, delaying equilibration between the cell body and ciliary pools of soluble tubulin. Because of this delay, we hypothesize that diffusion alone is insufficient to supply new tubulin to the cilium fast enough to support axonemal assembly during phases of rapid ciliary growth. If correct, a quickly polymerizing axoneme embedded in a small volume of ciliary matrix could deplete soluble tubulin near the tip, causing tubulin to drop below the critical concentration for microtubule assembly, stalling elongation of the axoneme and potentially triggering depolymerization. IFT proteins are present on cytoplasmic microtubules radiating from the ciliary base (Brown et al., 2015; Ritchey and Qin, 2012; Wingfield et al., 2017) and IFT trains are assembled over an extended area around the basal bodies, likely allowing them to capture tubulin from this larger area, carry it through the transition zone and unload it near the ciliary tip (Brown et al., 2015; Wingfield et al., 2017). Thus, IFT will likely overcome the limitations of tubulin entry by diffusion originating from the narrowness of the transition zone (Schuss et al., 2007). Even with the bulk of axonemal tubulin entering cilia by diffusion, motor-based IFT could maintain the concentration of tubulin near the tip above a threshold critical for efficient axonemal assembly and cilia elongation, thereby ensuring rapid uninterrupted axonemal growth. Further experimentation should be able to test this hypothesis.

MATERIALS AND METHODS

Strains and culture conditions

Chlamydomonas reinhardtii was maintained in modified M medium at room temperature, aeration with 0.5% CO₂, and a light/dark cycle of 14:10 h (Witman, 1986). Strain CC-620 was used as wild type for most experiments; other strains used included *ift72-2 IFT74 Δ 130* and *ift81-1 IFT81-CH5E* (Kubo et al., 2016) (<http://www.chlamycollection.org/>).

Generation of transgenic strains

The *TUB2* gene encoding β -tubulin was synthesized omitting the second intron and introducing flanking BamHI and EcoRI sites (Genewiz). The *TUA1* gene in the previously described vector pBR25-sfGFP- α -tubulin (Craft et al., 2015; Rasala et al., 2013) was replaced with the modified *TUB2* using digestion with BamHI and EcoRI and ligation. Changes in the sequence encoding the E-hook of β -tubulin were prepared as follows: gene segments encoding the modified C termini (E-hooks) of β -tubulin were synthesized (Genewiz), excised with EcoRI and EcoRV, and ligated into the pBR25-sfGFP vector digested with the same enzymes, taking advantage of a unique EcoRV site near the 3' end of the *TUB2* gene. Plasmids were restricted with KpnI and XbaI, and a fragment encompassing the functional Ble::GFP- β -tubulin cassette was gel purified and transformed into the various *C. reinhardtii* strains by electroporation. TAP plates (<https://www>.

chlamycollection.org/methods/media-recipes/tap-and-tris-minimal/) with 10 µg/ml zeocin were used to select transformants. Transformant colonies were transferred to liquid media in 96-well plates and screened by total internal reflection fluorescence (TIRF) microscopy for expression of GFP. Expression of GFP- α -tubulin has been described previously (Craft et al., 2015). The *ift20-1* IFT20-mCherry strain was transformed with the construct encoding sGFP- β -tubulin to obtain a double-tagged strain (Lechtreck et al., 2009).

Isolation and fractionation of cilia

To isolate cilia for biochemical analysis we followed the protocol by Witman (1986). Cells were concentrated by centrifugation (1150 g, 3 min, room temperature) and washed with 10 mM HEPES, pH 7.4. Cells were resuspended in HMS (10 mM HEPES, 5 mM MgSO₄ and 4% sucrose) and deciliated by the addition dibucaine (final concentration of 4.17 mM; Sigma-Aldrich) and vigorous pipetting. The cell bodies were removed by centrifugation and cilia were sedimented (17,000 g, 4°C, 20 min). Isolated cilia were resuspended in a microtubule-stabilizing buffer, HMEK (30 mM HEPES, 5 mM MgSO₄, 0.5 mM EGTA and 25 mM KCl) plus protease inhibitor (P9599; 1:100; Sigma-Aldrich), and demembrated by addition of NP-40 Alternative (1% final concentration; EMD Millipore) on ice for 20 min. Axonemes were separated from the membrane and matrix fraction by centrifugation (30,000 g, 4°C, 20 min) and fractions were analyzed using SDS-PAGE and western blotting.

Western blotting

Ciliary proteins were separated using SDS-PAGE and transferred to PVDF membrane (Immobilon; Millipore). The following primary antibodies were used: rabbit anti-*Chlamydomonas*- β -tubulin (1:2000; a kind gift from Joel Rosenbaum, Yale University, New Haven, CT; Silflow and Rosenbaum, 1981), mouse monoclonal anti-IC2 (1:50; King and Witman, 1990), rabbit anti-GFP (1:500; Invitrogen), and rabbit anti-NAB1 (1:5000; Agrisera). Western blots were developed using anti-mouse or anti-rabbit secondary antibodies conjugated to horseradish peroxidase (Molecular Probes) and chemiluminescence substrate (SuperSignal West Dura; Thermo Fisher Scientific). A ChemiDoc MP imaging system was used for imaging, and Image Lab (both Bio-Rad Laboratories) was used for signal quantification via densitometry.

Ciliary regeneration

Cells were washed and resuspended in M medium, deciliated by a pH shock (pH ~4.2 for 45 s), transferred to fresh M medium, and allowed to regrow cilia under constant light with agitation (Lefebvre, 1995). To delay the onset of regeneration, cells were kept on ice until needed. To initiate regeneration, cells were diluted into ambient temperature M medium.

In vivo microscopy

For *in vivo* imaging of GFP-tubulin by through-the-objective TIRF illumination, we used a Nikon Eclipse Ti-U equipped with a 60 \times NA1.49 objective and 40-mW 488-nm and 75-mW 561-nm diode lasers (Spectraphysics; Lechtreck, 2013, 2016). The excitation lasers were cleaned up with a Nikon GFP/mCherry TIRF filter and the emission was separated using an image splitting device (Photometrics DualView2 with filter cube 11-EM). Specimens were prepared as follows. Cells (~10 µl) were placed inside a ring of vacuum grease onto a 24 \times 60 mm No. 1.5 cover glass and allowed to settle (~1–3 min). The observation chamber was closed by inverting a 22 \times 22 mm No. 1.5 cover glass with ~10 µl of 5 mM HEPES pH 7.3, 5 mM EGTA onto the larger cover glass. Images were recorded at 10–40 f.p.s. using an iXON3 camera (Andor) and the NIS-Elements Advanced Research software (Nikon). To image structures located deeper in the cell body, such as cytoplasmic microtubules (Fig. 1B panels d and e), we used a smaller incident angle, allowing the light to penetrate deeper into the specimen. ImageJ (National Institutes of Health) with the LOCI plugin (University of Wisconsin, Madison WI) and multiple kymogram plugin (European Molecular Biology Laboratory) were used to generate kymograms as previously described (Lechtreck, 2013). To photobleach the cilia, the intensity of the 488-nm laser was increased to ~10% for 4–12 s; alternatively, a ciliary segment was bleached using a focused laser beam

moved by a motorized steering mirror. To image diffusing GFP-tubulin at high frame rates, laser intensity was increased to 10–50%.

Video analysis

IFT transport events were identified manually in ImageJ. The angle tool was used to determine the velocity of the transport events. Data were transferred to Microsoft Excel for further analysis. If not stated differently in the figure legend, the *n* values state the number of cilia analyzed. Individual frames and kymograms were saved in ImageJ, Adobe Photoshop was used to adjust brightness and contrast, and figures were mounted in Illustrator.

Acknowledgements

We thank Joel Rosenbaum (Yale University) for the kind gift of anti-*Chlamydomonas*- β -tubulin).

Competing interests

The authors declare no competing or financial interests.

Author contributions

Conceptualization: K.F.L.; Methodology: J.C.V.D.W., J.A.H., T.K., G.B.W., K.F.L.; Formal analysis: J.C.V.D.W., J.A.H., T.K.; Investigation: J.C.V.D.W., J.A.H., T.K., K.F.L.; Resources: T.K.; Writing - original draft: J.C.V.D.W., J.A.H., T.K., G.B.W., K.F.L.; Writing - review & editing: G.B.W., K.F.L.; Visualization: J.C.V.D.W., J.A.H.; Supervision: G.B.W., K.F.L.; Funding acquisition: G.B.W., K.F.L.

Funding

This study was supported by a Uehara Memorial Foundation Research Fellowship for Research Abroad (to T.K.), the Robert W. Booth Endowment at the University of Massachusetts Medical School (to G.B.W.), and grants by the National Institutes of Health (R37GM030626 and R35GM122574 to G.B.W. and R01GM110413 to K.F.L.). The content is solely the responsibility of the authors and does not necessarily represent the official views of the National Institutes of Health. Deposited in PMC for release after 12 months.

Supplementary information

Supplementary information available online at <https://jcs.biologists.org/lookup/doi/10.1242/jcs.249805.supplemental>

References

- Ahmed, N. T., Gao, C., Lucker, B. F., Cole, D. G. and Mitchell, D. R. (2008). ODA16 aids axonemal outer row dynein assembly through an interaction with the intraflagellar transport machinery. *J. Cell Biol.* **183**, 313–322. doi:10.1083/jcb.200802025
- Awata, J., Takada, S., Standley, C., Lechtreck, K. F., Bellve, K. D., Pazour, G. J., Fogarty, K. E. and Witman, G. B. (2014). NPHP4 controls ciliary trafficking of membrane proteins and large soluble proteins at the transition zone. *J. Cell Sci.* **127**, 4714–4727. doi:10.1242/jcs.155275
- Badgandi, H. B., Hwang, S. H., Shimada, I. S., Lorient, E. and Mukhopadhyay, S. (2017). Tubby family proteins are adaptors for ciliary trafficking of integral membrane proteins. *J. Cell Biol.* **216**, 743–760. doi:10.1083/jcb.201607095
- Berbari, N. F., Lewis, J. S., Bishop, G. A., Askwith, C. C. and Mykityn, K. (2008). Bardet-Biedl syndrome proteins are required for the localization of G protein-coupled receptors to primary cilia. *Proc. Natl. Acad. Sci. USA* **105**, 4242–4246. doi:10.1073/pnas.0711027105
- Bhogaraju, S., Cajanek, L., Fort, C., Blisnick, T., Weber, K., Taschner, M., Mizuno, N., Lamla, S., Bastin, P., Nigg, E. A. et al. (2013). Molecular basis of tubulin transport within the cilium by IFT74 and IFT81. *Science* **341**, 1009–1012. doi:10.1126/science.1240985
- Bhogaraju, S., Weber, K., Engel, B. D., Lechtreck, K. F. and Lorentzen, E. (2014). Getting tubulin to the tip of the cilium: one IFT train, many different tubulin cargo-binding sites? *BioEssays* **36**, 463–467. doi:10.1002/bies.201400007
- Billker, O., Shaw, M. K., Jones, I. W., Ley, S. V., Mordue, A. J. and Sinden, R. E. (2002). Azadirachtin disrupts formation of organised microtubule arrays during microgametogenesis of *Plasmodium berghei*. *J. Eukaryot. Microbiol.* **49**, 489–497. doi:10.1111/j.1550-7408.2002.tb00234.x
- Borisy, G. G. and Taylor, E. W. (1967). The mechanism of action of colchicine. Binding of colchicine-3H to cellular protein. *J. Cell Biol.* **34**, 525–533. doi:10.1083/jcb.34.2.525
- Breslow, D. K., Koslover, E. F., Seydel, F., Spakowitz, A. J. and Nachury, M. V. (2013). An *in vitro* assay for entry into cilia reveals unique properties of the soluble diffusion barrier. *J. Cell Biol.* **203**, 129–147. doi:10.1083/jcb.201212024
- Briggs, L. J., Davidge, J. A., Wickstead, B., Ginger, M. L. and Gull, K. (2004). More than one way to build a flagellum: comparative genomics of parasitic protozoa. *Curr. Biol.* **14**, R611–R612. doi:10.1016/j.cub.2004.07.041

- Brown, J. M., Cochran, D. A., Craige, B., Kubo, T. and Witman, G. B.** (2015). Assembly of IFT trains at the ciliary base depends on IFT74. *Curr. Biol.* **25**, 1583-1593. doi:10.1016/j.cub.2015.04.060
- Carminati, J. L. and Stearns, T.** (1997). Microtubules orient the mitotic spindle in yeast through dynein-dependent interactions with the cell cortex. *J. Cell Biol.* **138**, 629-641. doi:10.1083/jcb.138.3.629
- Cole, D. G., Diener, D. R., Himelblau, A. L., Beech, P. L., Fuster, J. C. and Rosenbaum, J. L.** (1998). Chlamydomonas kinesin-II-dependent intraflagellar transport (IFT): IFT particles contain proteins required for ciliary assembly in *Caenorhabditis elegans* sensory neurons. *J. Cell Biol.* **141**, 993-1008. doi:10.1083/jcb.141.4.993
- Craft, J. M., Harris, J. A., Hyman, S., Kner, P. and Lechtreck, K. F.** (2015). Tubulin transport by IFT is upregulated during ciliary growth by a cilium-autonomous mechanism. *J. Cell Biol.* **208**, 223-237. doi:10.1083/jcb.201409036
- Dai, J., Barbieri, F., Mitchell, D. R. and Lechtreck, K. F.** (2018). In vivo analysis of outer arm dynein transport reveals cargo-specific intraflagellar transport properties. *Mol. Biol. Cell* **29**, 2553-2565. doi:10.1091/mbc.E18-05-0291
- Dentler, W.** (2005). Intraflagellar transport (IFT) during assembly and disassembly of Chlamydomonas flagella. *J. Cell Biol.* **170**, 649-659. doi:10.1083/jcb.200412021
- Duan, J. and Gorovsky, M. A.** (2002). Both carboxy-terminal tails of α - and β -tubulin are essential, but either one will suffice. *Curr. Biol.* **12**, 313-316. doi:10.1016/S0960-9822(02)00651-6
- Hao, L., Thein, M., Brust-Mascher, I., Civelekoglu-Scholey, G., Lu, Y., Acar, S., Prevo, B., Shaham, S. and Scholey, J. M.** (2011). Intraflagellar transport delivers tubulin isoforms to sensory cilium middle and distal segments. *Nat. Cell Biol.* **13**, 790-798. doi:10.1038/ncb2268
- Harris, J. A., Liu, Y., Yang, P., Kner, P. and Lechtreck, K. F.** (2016). Single-particle imaging reveals intraflagellar transport-independent transport and accumulation of EB1 in Chlamydomonas flagella. *Mol. Biol. Cell* **27**, 295-307. doi:10.1091/mbc.e15-08-0608
- Hou, Y. and Witman, G. B.** (2017). The N-terminus of IFT46 mediates intraflagellar transport of outer arm dynein and its cargo-adaptor ODA16. *Mol. Biol. Cell* **28**, 2420-2433. doi:10.1091/mbc.e17-03-0172
- Huh, W. K., Falvo, J. V., Gerke, L. C., Carroll, A. S., Howson, R. W., Weissman, J. S. and O'Shea, E. K.** (2003). Global analysis of protein localization in budding yeast. *Nature* **425**, 686-691. doi:10.1038/nature02026
- Hunter, E. L., Lechtreck, K., Fu, G., Hwang, J., Lin, H., Gokhale, A., Alford, L. M., Lewis, B., Yamamoto, R., Kamiya, R. et al.** (2018). The IDA3 adapter, required for IFT transport of I1 dynein, is regulated by ciliary length. *Mol. Biol. Cell* **29**, 886-896. doi:10.1091/mbc.E17-12-0729
- Jordan, M. A., Diener, D. R., Stepanek, L. and Pigino, G.** (2018). The cryo-EM structure of intraflagellar transport trains reveals how dynein is inactivated to ensure unidirectional anterograde movement in cilia. *Nat. Cell Biol.* **20**, 1250-1255. doi:10.1038/s41556-018-0213-1
- Kee, H. L., Dishinger, J. F., Blasius, T. L., Liu, C. J., Margolis, B. and Verhey, K. J.** (2012). A size-exclusion permeability barrier and nucleoporins characterize a ciliary pore complex that regulates transport into cilia. *Nat. Cell Biol.* **14**, 431-437. doi:10.1038/ncb2450
- Kee, H. L. and Verhey, K. J.** (2013). Molecular connections between nuclear and ciliary import processes. *Cilia* **2**, 11. doi:10.1186/2046-2530-2-11
- King, S. M. and Witman, G. B.** (1990). Localization of an intermediate chain of outer arm dynein by immunoelectron microscopy. *J. Biol. Chem.* **265**, 19807-19811.
- Kozminski, K. G., Johnson, K. A., Forscher, P. and Rosenbaum, J. L.** (1993). A motility in the eukaryotic flagellum unrelated to flagellar beating. *Proc. Natl. Acad. Sci. USA* **90**, 5519-23. doi:10.1073/pnas.90.12.5519
- Kubo, T., Brown, J. M., Bellve, K., Craige, B., Craft, J. M., Fogarty, K., Lechtreck, K. F. and Witman, G. B.** (2016). The IFT81 and IFT74 N-termini together form the major module for intraflagellar transport of tubulin. *J. Cell Sci.* **129**, 2106-2119. doi:10.1242/jcs.187120
- Lechtreck, K. F.** (2013). In vivo imaging of IFT in Chlamydomonas flagella. *Methods Enzymol.* **524**, 265-284. doi:10.1016/B978-0-12-397945-2.00015-9
- Lechtreck, K. F.** (2016). Methods for studying movement of molecules within cilia. *Methods Mol. Biol.* **1454**, 83-96. doi:10.1007/978-1-4939-3789-9_6
- Lechtreck, K. F., Brown, J. M., Sampaio, J. L., Craft, J. M., Shevchenko, A., Evans, J. E. and Witman, G. B.** (2013). Cycling of the signaling protein phospholipase D through cilia requires the BBSome only for the export phase. *J. Cell Biol.* **201**, 249-261. doi:10.1083/jcb.201207139
- Lechtreck, K. F., Johnson, E. C., Sakai, T., Cochran, D., Ballif, B. A., Rush, J., Pazour, G. J., Ikebe, M. and Witman, G. B.** (2009). The Chlamydomonas reinhardtii BBSome is an IFT cargo required for export of specific signaling proteins from flagella. *J. Cell Biol.* **187**, 1117-1132. doi:10.1083/jcb.200909183
- Lefebvre, P. A.** (1995). Flagellar amputation and regeneration in Chlamydomonas. *Methods Cell Biol.* **47**, 3-7. doi:10.1016/S0091-679X(08)60782-7
- Lin, Y. C., Niewiadomski, P., Lin, B., Nakamura, H., Phua, S. C., Jiao, J., Levchenko, A., Inoue, T. and Rohatgi, R.** (2013). Chemically inducible diffusion trap at cilia reveals molecular sieve-like barrier. *Nat. Chem. Biol.* **9**, 437-443. doi:10.1038/nchembio.1252
- Luo, W., Ruba, A., Takao, D., Zweifel, L. P., Lim, R. Y. H., Verhey, K. J. and Yang, W.** (2017). Axonemal lumen dominates cytosolic protein diffusion inside the primary cilium. *Sci. Rep.* **7**, 15793. doi:10.1038/s41598-017-16103-z
- Madey, P. and Melkonian, M.** (1990). Flagellar development during the cell cycle in Chlamydomonas reinhardtii. *Botanica Acta* **103**, 97-102. doi:10.1111/j.1438-8677.1990.tb00133.x
- Marshall, W. F. and Rosenbaum, J. L.** (2001). Intraflagellar transport balances continuous turnover of outer doublet microtubules: implications for flagellar length control. *J. Cell Biol.* **155**, 405-414. doi:10.1083/jcb.200106141
- Nielsen, M. G., Turner, F. R., Hutchens, J. A. and Raff, E. C.** (2001). Axoneme-specific β -tubulin specialization: a conserved C-terminal motif specifies the central pair. *Curr. Biol.* **11**, 529-533. doi:10.1016/S0960-9822(01)00150-6
- Rasala, B. A., Barrera, D. J., Ng, J., Plucinak, T. M., Rosenberg, J. N., Weeks, D. P., Oylar, G. A., Peterson, T. C., Haerizadeh, F. and Mayfield, S. P.** (2013). Expanding the spectral palette of fluorescent proteins for the green microalga Chlamydomonas reinhardtii. *Plant J.* **75**, 545-556. doi:10.1111/tpj.12165
- Richey, E. A. and Qin, H.** (2012). Dissecting the sequential assembly and localization of intraflagellar transport particle complex B in Chlamydomonas. *PLoS ONE* **7**, e43118. doi:10.1371/journal.pone.0043118
- Ringo, D. L.** (1967). Flagellar motion and fine structure of the flagellar apparatus in Chlamydomonas. *J. Cell Biol.* **33**, 543-571. doi:10.1083/jcb.33.3.543
- Rosenbaum, J. L., Moulder, J. E. and Ringo, D. L.** (1969). Flagellar elongation and shortening in Chlamydomonas. The use of cycloheximide and colchicine to study the synthesis and assembly of flagellar proteins. *J. Cell Biol.* **41**, 600-619. doi:10.1083/jcb.41.2.600
- Schuss, Z., Singer, A. and Holcman, D.** (2007). The narrow escape problem for diffusion in cellular microdomains. *Proc. Natl. Acad. Sci. USA* **104**, 16098-16103. doi:10.1073/pnas.0706599104
- Siffow, C. D. and Rosenbaum, J. L.** (1981). Multiple alpha- and beta-tubulin genes in Chlamydomonas and regulation of tubulin mRNA levels after deflagellation. *Cell* **24**, 81-88. doi:10.1016/0092-8674(81)90503-1
- Taschner, M., Weber, K., Mourao, A., Vetter, M., Awasthi, M., Stiegler, M., Bhogaraju, S. and Lorentzen, E.** (2016). Intraflagellar transport proteins 172, 80, 57, 54, 38, and 20 form a stable tubulin-binding IFT-B2 complex. *EMBO J.* **35**, 773-790. doi:10.15252/embj.201593164
- Thazhath, R., Liu, C. and Gaertig, J.** (2002). Polyglycylation domain of beta-tubulin maintains axonemal architecture and affects cytokinesis in Tetrahymena. *Nat. Cell Biol.* **4**, 256-259. doi:10.1038/ncb764
- van Dam, T. J. P., Townsend, M. J., Turk, M., Schlessinger, A., Sali, A., Field, M. C. and Huynen, M. A.** (2013). Evolution of modular intraflagellar transport from a coatomer-like progenitor. *Proc. Natl. Acad. Sci. USA* **110**, 6943-6948. doi:10.1073/pnas.1221011110
- Wingfield, J. L., Mengoni, I., Bomberger, H., Jiang, Y.-Y., Walsh, J. D., Brown, J. M., Picariello, T., Cochran, D. A., Zhu, B., Pan, J. et al.** (2017). IFT trains in different stages of assembly queue at the ciliary base for consecutive release into the cilium. *Elife* **6**, e26609. doi:10.7554/eLife.26609
- Witman, G. B.** (1986). Isolation of Chlamydomonas flagella and flagellar axonemes. *Methods Enzymol.* **134**, 280-290. doi:10.1016/0076-6879(86)34096-5
- Xia, L., Hai, B., Gao, Y., Burnette, D., Thazhath, R., Duan, J., Bre, M. H., Levilliers, N., Gorovsky, M. A. and Gaertig, J.** (2000). Polyglycylation of tubulin is essential and affects cell motility and division in Tetrahymena thermophila. *J. Cell Biol.* **149**, 1097-1106. doi:10.1083/jcb.149.5.1097
- Zhu, X., Liang, Y., Gao, F. and Pan, J.** (2017). IFT54 regulates IFT20 stability but is not essential for tubulin transport during ciliogenesis. *Cell. Mol. Life Sci.* **74**, 3425-3437. doi:10.1007/s00018-017-2525-x

Supplementary material

Supplementary tables

protein	variant	C-terminal sequence	anterograde IFT ($\mu\text{m/s}$)	retrograde IFT ($\mu\text{m/s}$)	Swimming ($\mu\text{m/s}$)
GFP- β -tubulin	WT E-hook	SAEEEGEFEGEEEEE*	2.2 (SD 0.5, n = 360)	2.45 (SD 1, n = 18)	86 (SD 24, n = 230)
GFP- β -tubulin	α E-hook	SAEGAGEGEGEEY*	2.13 (SD 0.44, n = 33)	2.7 (SD 0.5, n = 5)	75 (SD 19, n = 163)
GFP- β -tubulin	-5E-hook	SAEEEGAFAGAAEA*	1.95 (SD 0.49, n = 71)	2.8 (SD 1.3, n = 16)	70 (SD 21, n = 146)
GFP- β -tubulin	Δ E-hook	SA*	2.29 (SD 0.45, n = 50)	2.9 (SD 1.2, n = 69)	80 (SD 22, n = 235)
GFP- α -tubulin	WT E-hook	LEKDFEEVGAAESAEGAGEGEGEEY*	2.09 (SD 0.35, n = 27)	<u>n.d.</u>	<u>n.d.</u>
GFP- α -tubulin	Δ E-hook	LEKDFEEVGAEY*	1.91 (SD 0.35, n = 20)	<u>n.d.</u>	<u>n.d.</u>

Table S1: Tubulin constructs used in this study

Sequences of the E-hooks of wild-type GFP α - and β -tubulin and the modified tubulin molecules. Transport velocities of the fusion proteins by IFT and the swimming velocities of the transformants are listed.

Supplementary figures

Figure S1

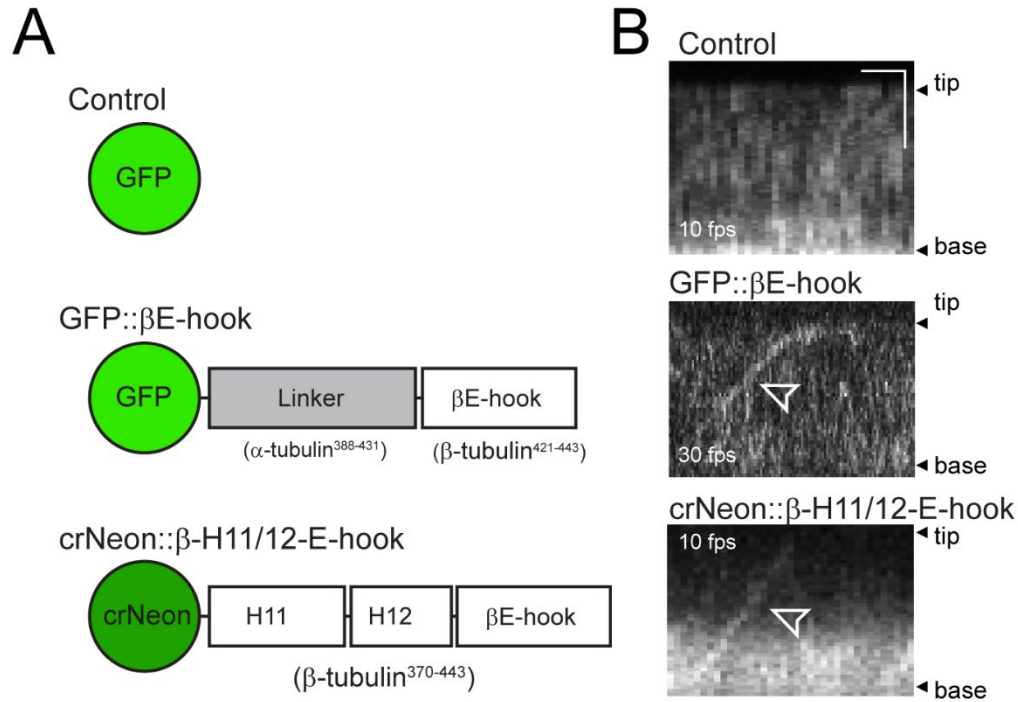


Fig. S1) The β E-hook is not sufficient to mediate high frequency transport of GFP by IFT

A) Schematic presentation of the construct fusing GFP or mNG to C-terminal regions of β -tubulin. H11, H12 refers to helix 11 and 12 of β -tubulin, which neighbor the E-hook.

B) Kymograms of the constructs shown in A. Note that the associated videos were recorded at different frame rates (fps). Bars = 1 s \times 2 μ m.

Figure S2

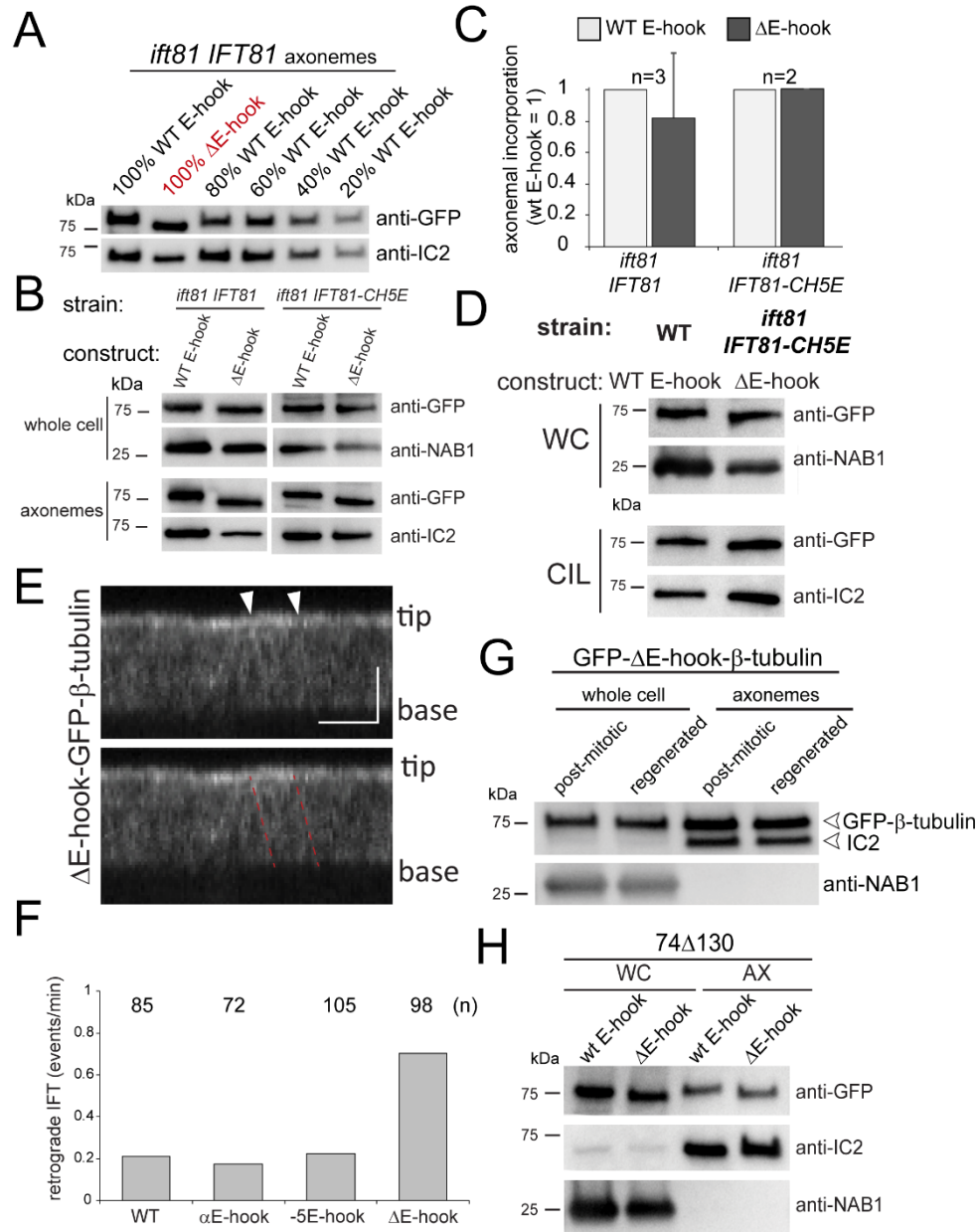


Figure S2) Transport and axonemal incorporation of E-hook-deficient β -tubulin

A) Western blot analysis of isolated axonemes of the *ift81-1 IFT81* strain expressing full-length (WT) or Δ E-hook GFP- β -tubulin. The wild-type samples were diluted as indicated and compared to the undiluted Δ E-hook β tubulin sample.

B) Western blot of the two *ift81-1* rescue strains comparing whole-cell and axoneme samples using anti-GFP and antibodies to NAB1 and IC2 as loading controls.

C) Histograms comparing the changes in the axonemal amounts of Δ E-hook vs. full-length β -tubulin in the *ift81-1 IFT81* and *ift81-1 IFT81-CH5E* rescue strains as quantified based on western blots probed with anti-GFP. The band intensities of the full-length GFP- β -tubulin in each back ground were set to 1. n, number of independent cilia isolates.

D) Western blot of whole-cell (WC) and cilia (CIL) samples comparing a control strain expressing full-length β -tubulin to an *ift81-1 IFT81-CH5E* strain expressing Δ E-hook-deficient β -tubulin side by side. The antibodies used are indicated.

E) Kymogram and replicate kymogram with marked tracks showing retrograde IFT of E-hook-deficient β -tubulin. Bars = 2 s 2 μ m.

F) Histogram showing the frequency of retrograde IFT for full-length (WT) and the modified β -tubulins in regenerating cilia. N, number of cilia analyzed.

G) Comparison of axonemes isolated from postmitotic and regenerated cilia and the corresponding whole cell samples. Regenerated cilia were isolated ~3 hours after the pH-shock; postmitotic cilia ~6 hours after the onset of the light. Antibodies to IC2 and NAB1 were used as loading controls.

H) Analysis of the distribution of GFP-tagged full-length and truncated β -tubulin in whole cell (WC) and axonemes (AX) of the *ift74-2 IFT74 Δ 130* strain. In this background, full-length and

truncated tubulin are transported with similar frequencies by IFT (Fig. 3C). Both full-length and truncated tubulin are incorporated in similar amounts into the axoneme suggesting that the incorporation of tubulin into the axoneme is not affected by the absence or presence of the β -tubulin E-hook. The strains selected for this experiment expressed GFP-tubulin at less than 2% of the total tubulin.

Figure S3) IFT and diffusion of GFP- β -tubulin near the ciliary tip

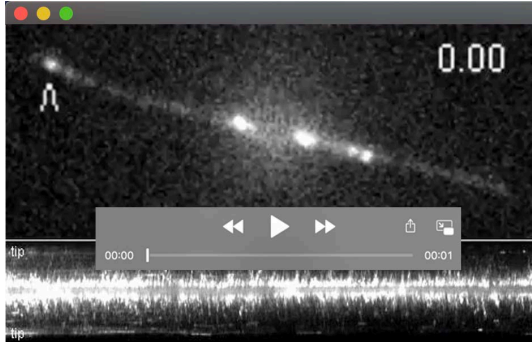
A) Gallery of kymograms showing the entry of GFP- β -tubulin into full-length cilia by diffusion (red arrows). Manual inspection of the kymograms suggests that these GFP- β -tubulin trajectories originate from individual entry events. Arrowhead, IFT. Based on movies recorded at 33 fps. Bars = 1 s 2 μ m.

B) Tubulin turnover at the tip of a full-length cilium. Still images showing a GFP- β -tubulin cilium prior to, immediately after, and 20 s after photobleaching of the distal segment. The corresponding kymogram is shown on the right. Note signal recovery in two spots near the ciliary tip. Bar = 1 s 2 μ m.

C) Four kymograms of full-length (a, b) and regenerating (c, d) cilia of cells expressing full-length (a, c) or Δ E-GFP- β -tubulin (b, d) in wild-type cells. Cilia were bleached repeatedly and allowed to recover. Note the recovery of a bright signal at the tips (black arrowheads marked T) of the growing cilia due to the incorporation of full-length and truncated GFP- β -tubulin. Open arrowheads, IFT trajectories. Open arrows indicate diffusion of GFP- β -tubulin. The diagonal traces visible during some of the bleaching steps show the laser beam moving up and down the cilium (see movie S2). Based on movies recorded at 10 fps. Bars (in a for a – d) = 2 s 2 μ m.

D) Gallery of kymograms showing the re-entry of GFP- β -tubulin by diffusion (arrows) and IFT (open arrowheads) into the bleached distal segment of growing cilia. Note immobilization of some GFP- β -tubulin particles at the ciliary tip. Green arrow, putative bleaching event. Based on movies recorded at 20 fps (a, b) and 40 fps (c, d). Bars = 2 s 2 μ m.

Supplementary Movies



Movie S1) Rapid entry of GFP- β -tubulin into cilia by diffusion.

The movie shows a wild-type cell with full-length cilia expressing GFP- β -tubulin and was recorded at 20 fps; the corresponding kymogram is shown below. The left ciliary tip is marked by an arrowhead. The timer displays seconds.ms.



Movie S2) Partial bleaching of cilia

The movie depicts a wild-type GFP- β -tubulin cell with regenerating cilia; the corresponding kymogram is shown below. For FRAP analysis, the distal ciliary segment was bleached using a focused laser beam. Note re-entry of GFP- β -tubulin into the bleached segment including numerous IFT events. The movie was recorded at 20fps and the timer show seconds.ms.